New Zealand Journal of Geology and Geophysics, 1998, Vol. 41: 39–49
0028–8306/98/4101–0039 $7.00/0

Crustal structure in the central South Island, New Zealand, from the Lake Pukaki seismic experiment

STEFAN KLEFFMANN[1]
FRED DAVEY[2]
ANNE MELHUISH[2]
DAVID OKAYA[3]
TIM STERN[1]
and the SIGHT Team[4]

[1]Institute of Geophysics
Victoria University of Wellington
P.O. Box 600
Wellington, New Zealand

[2]Institute of Geological & Nuclear Sciences
P.O. Box 1320
Wellington, New Zealand

[3]University of Southern California
University Park
Los Angeles, CA 90089–0740
U.S.A.

[4]South Island GeopHysical Transect working group

Abstract The crustal structure of the central South Island, New Zealand, has been investigated using explosion seismology measurements. A series of 114 shots were fired in Lake Pukaki and recorded in three modes: on a 120 channel, 6 km long, seismic reflection array rolled along a 27 km profile on the eastern margin of Lake Pukaki; on a Reftek seismograph array consisting of 40 units spread over a 52 km long line, partially coincident with the reflection profile; and wide angle reflections from the lower crust recorded on permanent stations of the New Zealand Seismograph Network that were located between 80 and 120 km from the shots. The data show that the greywacke-schist forming the mid–upper crust of the Pacific plate is c. 25 km thick near the east coast and thickens as a crustal root to >35 km beneath the Southern Alps. A strong reflection was recorded from a depth of 25 km and is interpreted to be from the base of the greywacke-schist crust overlying an old oceanic crust.

Below 6 km depth the compressional seismic velocity is relatively uniform and increases only slightly from 6.2 km/s to 6.25 km/s at the lower crustal interface. A relatively large velocity gradient of 0.22 (km/s)/km is derived for the upper 6 km of the greywacke basement. Whether this velocity gradient, derived from a relatively short profile, is regional in extent needs to be verified. A Poisson's ratio of 0.21 ± 0.03 was determined from apparent velocities of Pg and Sg for the greywacke/schist and is interpreted to indicate fracturing in this layer.

Reflections, inferred to be from segments of the downdip extension of a broad Alpine Fault Zone, occur at depths of c. 22 and 28 km and indicate a dip of 33 ± 5°. A width of 7.5 km is estimated for the fault zone at this depth. The dipping reflector segments would intercept the surface west of the Alpine Fault, and suggest that the fault zone is steeper at shallower depths.

The total amount of material, which has been subjected to uplift, has been estimated from the amount of crustal shortening and the shape of the crustal root. These estimates indicate that 50% of this material has not been accounted for in previous studies, and suggests either a non-exponential distribution, or larger rates of uplift southeast of the Alpine Fault than thought previously.

Keywords crustal structure; active source seismology; tectonics; reflection; refraction; central South Island; Lake Pukaki

INTRODUCTION

Two seismic crustal structure experiments were carried out in the central South Island of New Zealand between February 1995 and March 1996. These experiments are part of a New Zealand – United States joint programme to study crustal structure and deformation at a continent-continent collisional zone (Henyey et al. 1993). This paper deals with the first phase of the seismic programme carried out in the McKenzie Basin along the eastern margin of Lake Pukaki (Fig. 1) in February 1995. The Lake Pukaki experiment was reconnaissance in character, and several seismic techniques were attempted.

Lake Pukaki was chosen for a pilot study of crustal structure in the central South Island for three principal reasons: (1) the proximity to the plate boundary; (2) the presence of the Bouguer gravity low; and (3) the long axis of the lake being at a high angle to the plate boundary. The latter provided the opportunity for locating the seismic profile nearly normal to the strike of the regional structure, using the lake for underwater shots and recording these on a seismic array that was placed along a gravel road which follows the eastern side of the lake (Fig. 1). Details of the surveying technique and preliminary data processing steps can be found in Melhuish & Kleffmann (1995).

Vertical incidence multichannel seismic reflection measurements (CMP) were carried out to image lower crustal targets. One hundred and fourteen 25 kg shots were fired at 2 or 4 km offsets into a 6 km long, 120 channel array (50 m group interval), resulting in a maximum shot receiver offset of 10 km.

G97002
Received 7 January 1997; accepted 9 October 1997

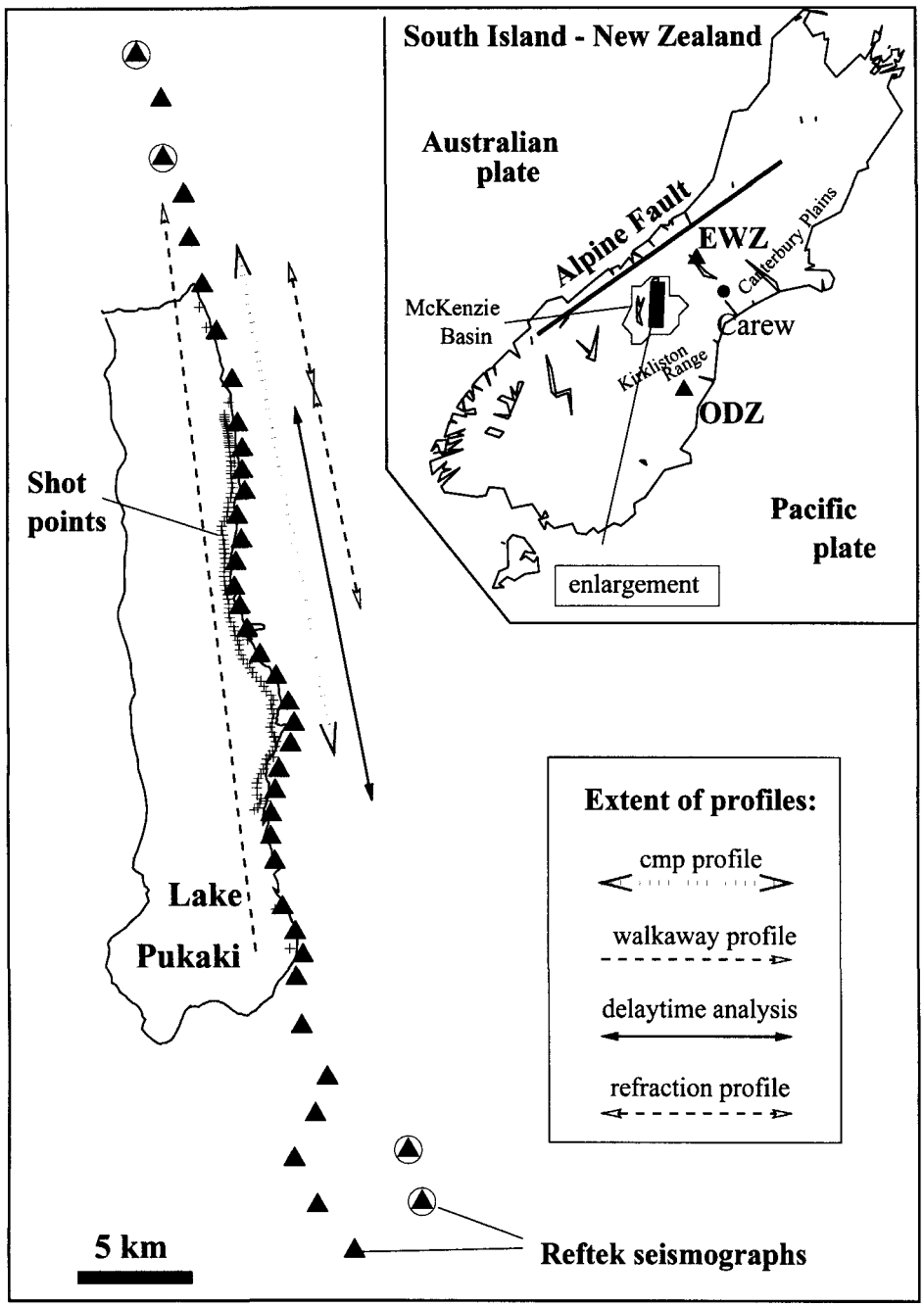

Fig. 1 Lake Pukaki survey area showing the locations of the Reftek seismographs (▲). Encircled stations are used to define a velocity gradient in the greywacke basement. Survey profiles are: a multi-channel reflection CMP line with a total length of 27 km; near-surface profiles obtained from shallow refraction recordings and delay-time analysis; and a walkaway spread. *Inset*: South Island of New Zealand with regional tectonic features. EWZ and ODZ are stations of the National Seismograph Network. The black rectangle defines the Lake Pukaki survey area.

Two supplementary seismic experiments were undertaken in the course of the multichannel experiment. Firstly, a walkaway experiment was carried out when the multichannel array was located at the northern end of the lake. Secondly, a seismic refraction study was made using 40 Reftek seismographs, which were deployed along the shore of the lake, with a total profile length of 52 km. In addition, a large number of the 114 lake shots were also recorded on two seismographs of the National Seismograph Network, at offset distances of 72 and 110 km, which provided important constraints on the lower crust.

In this paper these seismic data are described and the implications of their results for crustal structure presented.

GEOLOGY/TECTONICS

The plate boundary passes across New Zealand from the northeast to the southwest. The character of the plate boundary changes from west-dipping subduction of the Pacific plate along the eastern margin of the North Island (Australian plate), through continental collision in the central South Island, to an east-dipping subduction of the Australian plate under the southwestern South Island (Pacific plate).

Lake Pukaki is one of three glacial lakes in the McKenzie Basin in the central South Island (Fig. 1) which were formed during the last glaciation (Suggate et al. 1978). The McKenzie Basin has been shaped by several glacial periods (Speight 1963) and surficial glacial deposits dominate the

landforms (Gair 1967). To the northwest of the basin lies the Pacific-Australian plate boundary, which is most clearly manifest by the Alpine Fault. The Alpine Fault is a transform fault with primarily right-lateral movement (Wellman 1953). Relative movement between both plates has become increasingly oblique over the last 10 m.y. (Molnar et al. 1975; Walcott 1978; Pearson et al. 1995), resulting in a continent-continent collisional zone. Deformation has resulted in the creation of a major mountain chain, the Southern Alps. Current maximum uplift rates are believed to be of the order of 6–10 mm/yr (Wellman 1979; Kamp et al. 1989).

Wellman (1979) attributed the exposure of deep crustal schistose rocks east of the Alpine Fault to a delamination of the crust from the underlying mantle. The geometry of the deformation is not well constrained. Estimates of the burial depths of these mineral assemblages range from c. 13–21 km from fission track data (Kamp et al. 1989) to 19–25 km from thermobarometric data (Norris et al. 1990; Grapes 1995). Differences in the estimation of crustal thicknesses exist also between 2-D gravity models. The maximum negative Bouguer anomaly south of Mt Cook has been modelled by Woodward (1979) as a wedge-shaped crustal root with a maximum depth of 45 km, which contrasts with the model by Allis (1986) of broad crustal thickening with a maximum depth of 35 km. These discrepancies are due, in part, to uncertainty in the respective assumptions necessary to construct the models.

Seismicity studies associated with a seismograph network deployed around Lake Pukaki provided some constraints on crustal structure (Haines et al. 1979; Reyners 1987). Small magnitude earthquakes (M_l<4.0) occur at depths >50 km (Reyners 1987), and 1-D conversions of S–P phases have been related to an interface at a depth of c. 32 km inferred to be the Moho (Calhaem et al. 1977). A sparsely sampled refraction profile across the central South Island in 1983 (Smith et al. 1995) provided an upper crustal velocity structure, but the data were recorded at insufficient spatial intervals to resolve lower crustal units unambiguously.

By contrast, the seismic reflection data recorded from the Lake Pukaki seismic experiment place stringent depth constraints on the lower crust.

SEISMIC DATA AND INTERPRETATION

Near-surface structure

Seismic waves travelling through the surficial glacial deposits are attenuated by scattering and affected by spatially variable delays due to variations in velocity and thickness of the glacial layer. To estimate the time delays on the deep crustal data caused by the glacial surface layer, a detailed seismic image of the near-surface geology was derived from (1) two reversed refraction profiles, (2) first arrivals of the CMP line, and (3) first arrivals of the Reftek data.

The minimum offsets of 2 and 4 km, used for the CMP line, prevented the recording of direct waves as first arrivals, which resulted in a lack of control on near-surface velocities. This near-surface velocity information was provided by shooting two additional reversed refraction profiles near the northern end of the lake. The lengths of these profiles were extended with first arrival data recorded on shot gathers of the CMP line, which provided a continuous coverage of refraction data for most of the CMP profile (Fig. 1).

First arrivals indicate two distinct velocities on the refraction data (Fig. 2). These are identified as a surface velocity from the glacial till, which exhibits severe lateral variation, and a refractor velocity from the greywacke basement. Surface velocities are calculated from the refraction profiles using standard least-square methods. Velocities vary between 1790 and 2130 m/s (c. 15%). There is no correlation of velocities with location, that is, no increase in surface velocity towards either end of the lake is found. The scatter in velocity, which has also been identified in other studies (Kleffmann 1994), is attributed to the heterogeneous character of the glacial deposits. Lateral variations in the basement velocity are not apparent. Therefore, a simple 2-D inversion model with surface velocities varying linearly between shot locations (where they are defined), and a constant refractor velocity (4300 m/s), were chosen as appropriate to solve for the near-surface layer. The refractor boundary which results from this inversion (using the code from Zelt & Smith 1995) is shown in Fig. 2 (solid line). Depth values are plotted with respect to sea level. The thickness of the surface layer varies from 500 m at the southern end to c. 50 m at the northern end of the profile, thickening to c. 620 m in the middle. Maximum depth of the refractor is 120 m below sea level.

As picking errors are estimated to be minimal, the relatively large r.m.s. error of 34 ms between observed and calculated arrivaltimes is thought to be caused in part by projecting the crooked line onto a 1-D profile. An error must also be expected from the sparse lateral sampling of the basement refractor. Furthermore, the surface-layer velocities are not likely to vary smoothly along the profile. A velocity increase with depth in the basement refractor, as determined from the Reftek data (see below), does not alter this result significantly because differences in raypath curvature are small for the offsets used in the inversion.

Depths to the basement refractor below the shot locations were also calculated from first arrivals recorded on the Reftek seismographs, using the surface-consistent delaytime method described by Farrell & Euwema (1984). A smoothed refractor boundary is included in Fig. 2 (dashed line). Differences between the two depth models arise due to the assumption of vertically travelling rays in the delaytime analysis. The aim of the delaytime analysis is not to derive a true depth model, but to define surface-consistent time corrections which, when applied, result in a best-fit coherent reflection between CMP traces. Despite these limitations, the depth model derived from the delaytime approach is similar to the depth model obtained from the inversion process.

The two-layer model is not consistent with the geological cross-section proposed by Gair (1967), who assumed that Tertiary sediments underlie the glacial deposits in the McKenzie Basin. Measured velocities for Tertiary rock lie between the observed velocities for the glacial deposits and the velocities of the underlying greywacke basement (Langdale 1996). These are not observed on the refraction data, which indicates that Tertiary sediments are either thin or non-existent.

Reftek array

Data recorded on the Reftek array (Fig. 1) were used to determine the velocity structure of the upper crust. Picks of the refracted arrivals are plotted in Fig. 3 at a reduced

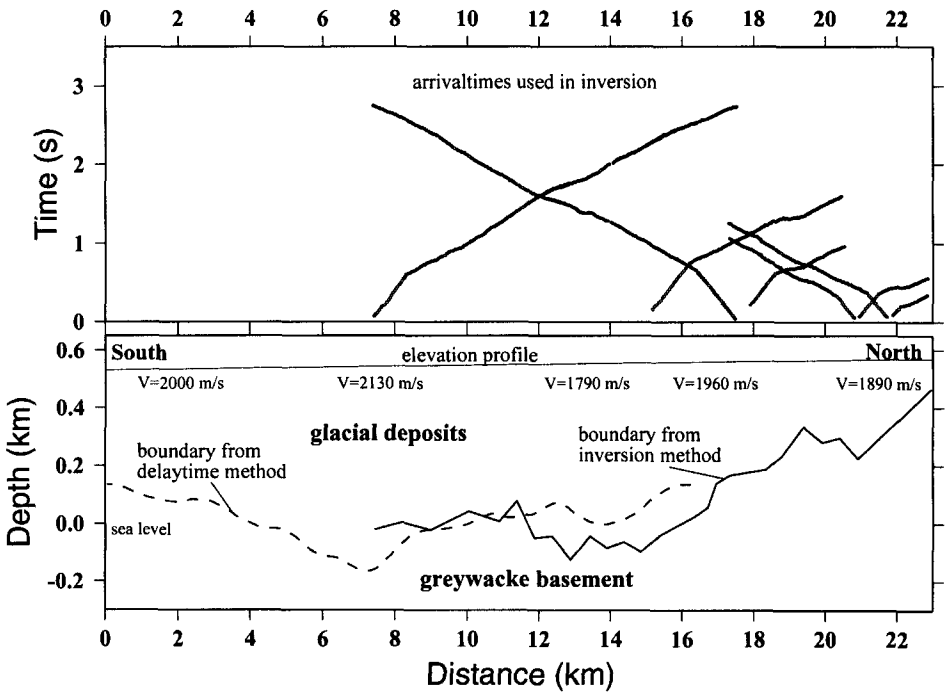

Fig. 2 A near-surface model from the Lake Pukaki experiment shows a thick sequence of glacial deposits with significant thinning of this layer towards the northern end of the lake. The refractor boundary is calculated using an inversion approach for the shallow refraction data, and by delaytime analysis of the Reftek data. The boundary obtained from the delaytime analysis is smoothed and limited to the extent of the shot array.

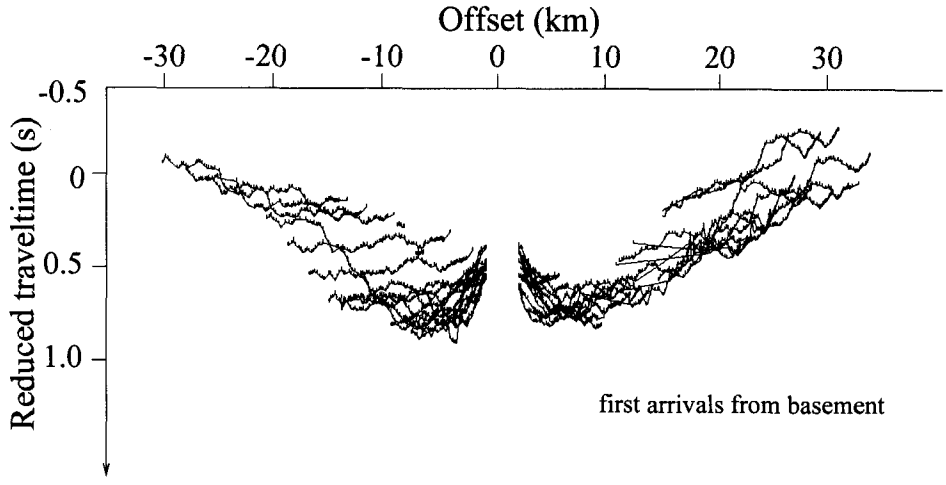

Fig. 3 First breaks from the basement refractor of the Reftek data are plotted versus offset at 5 km/s reduced traveltime. Negative and positive offsets represent distances to the south and north of the shotpoint, respectively. Time variations at any fixed offset result from shot and receiver statics.

velocity of 5 km/s. The curvature in the arrival lineation denotes a velocity gradient in the upper part of the greywacke basement. To generate a high-resolution velocity-depth model and derive the velocity gradient, a subset of these data was chosen. The main criteria were to establish maximum depth penetration of rays, which requires large shot-receiver offsets, and to minimise static and geometrical effects.

Two stations, which are on greywacke outcrop or close to it, were chosen at either end of the Reftek array. These four stations lie on an approximate straight line (stations are labelled by a circle in Fig. 1). Refracted arrivals recorded at these stations were used to derive a velocity gradient using the inversion programme from Zelt & Smith (1992). Errors introduced by projecting the shots onto this 2-D profile are minor.

For the inversion, the initial model assumed the near-surface layer defined by the shallow refraction and delaytime analysis. Differences in depth between both techniques were averaged. The depth profile of this layer was smoothed and a subset of depth points below the shot array was chosen. Since the surface-layer velocity is not well defined due to the heterogeneous character of the glacial deposits, a constant velocity of 2000 m/s was assumed. Initial forward raytracing steps were necessary to reduce short-wavelength undulations in the arrival pattern caused by uncertainties in this surface layer definition. The refractor boundary was carefully adjusted to give close agreement of observed and calculated arrival times. The refractor boundary (top of greywacke layer) was then fixed and the velocity gradient within the upper crust was computed by the inversion procedure. The inversion was constrained to give two velocity values at the

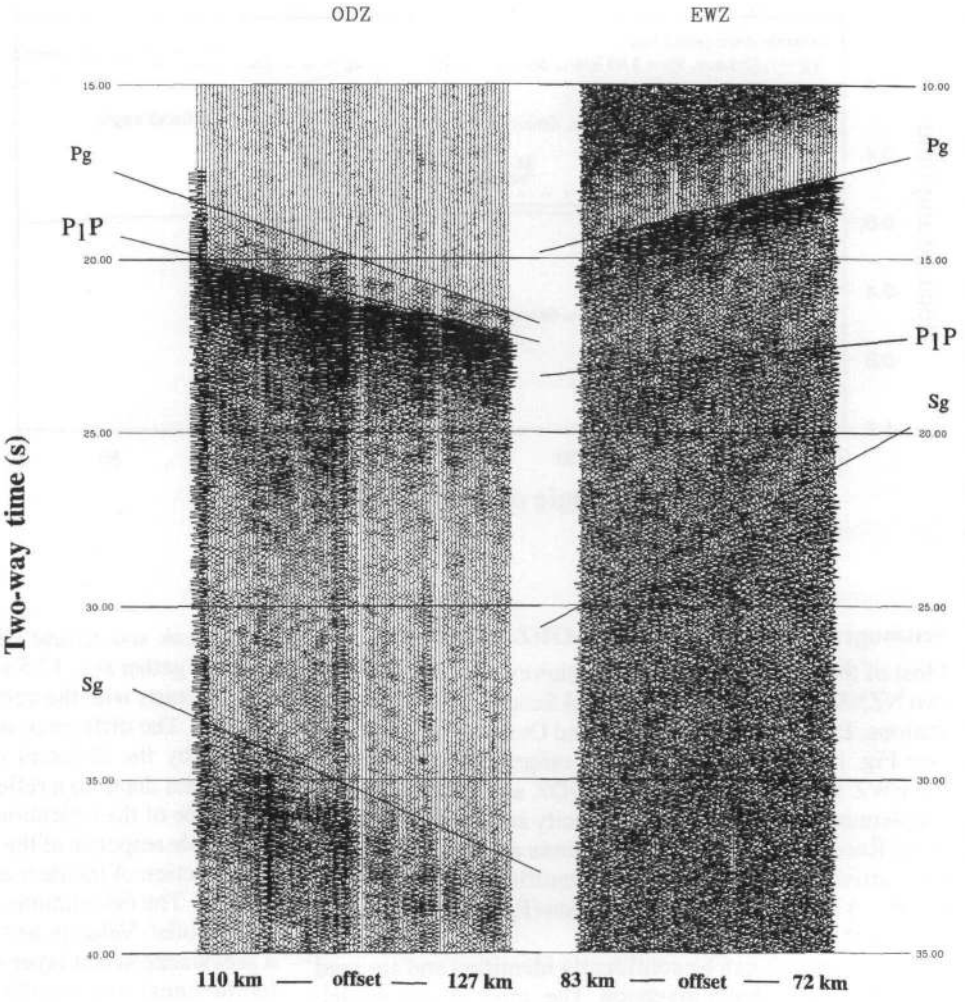

Fig. 4 Shots recorded by the National Seismograph Network at Erewhon (EWZ) and Otahau Downs (ODZ). A bandpass filter is applied and the traces are plotted at equidistant intervals. An AGC is applied to the EWZ receiver gather. The first arrivals of Pg and P_1P constrain the velocity of the greywacke crust. Direct S-wave arrivals are used to obtain estimates of Poisson's ratio.

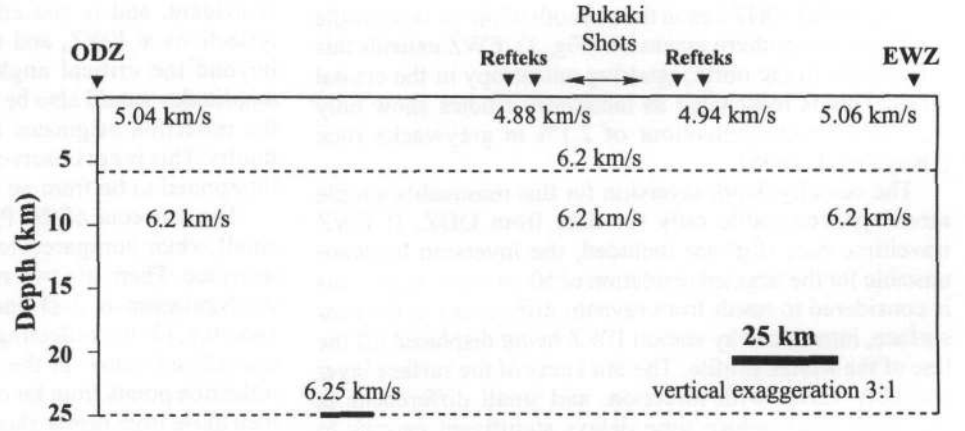

Fig. 5 The 2-D depth-velocity model of the greywacke crust derived from the inversion of first arrival data. The velocity increase from 4.9 km/s near the surface to 6.2 km/s at 6 km depth is determined from refracted arrivals at four Reftek stations north and south of Lake Pukaki. Below 6 km depth the velocity increases slightly to 6.25 km/s at 25 km depth. This lower interface is defined by the P_1P arrival at ODZ.

top of the basement at either end of the profile, allowing for lateral variation in the refractor velocity due to different degrees of surface weathering, and a third velocity value at maximum depth sampled by the data. The final model gives a velocity of 4.88–4.94 km/s below the receiver stations, which increases to 6.2 km/s at a depth of 6 km (see Fig. 5). This equates to a velocity gradient of 0.22 (km/s)/km. The r.m.s. error of 31 ms between calculated and observed arrivaltimes indicates a high resolution of seismic velocities. For example, changing the lower refractor velocity by 3% increases the r.m.s. error by a factor of 2. The r.m.s. error is similar to the r.m.s. error determined in the near-surface analysis, which suggest that the traveltime residuals are caused mainly in the glacial surface layer.

The basement velocity of 4.3 km/s derived from the shallow refraction survey is much lower than the minimum velocity value derived in this inversion. We consider this discrepancy to be a result of offset dependence of velocity, with a larger minimum offset in the inversion compared to the shallow refraction profile. It is likely that the velocity increase is nonlinear with a larger gradient near the surface.

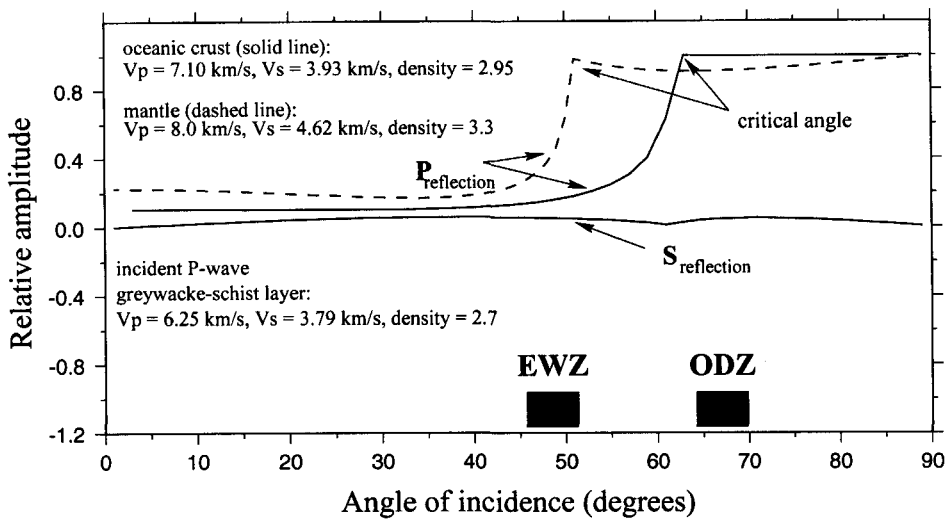

Fig. 6 Relative amplitude response of the lower crustal reflection is plotted versus angle of incidence. Calculations are based on a two-layer model using Zoeppritz's equations. Values used in the calculations are shown in the figure. Solid lines represent the amplitude response for a reflection from an oceanic crust for P and S phases. Dashed line shows the calculated response for a reflection from Moho (PmP). Offset distances of ODZ and EWZ are plotted with respect to their sampling of ray angles.

Seismograph network stations—ODZ and EWZ

Most of the shots from the Pukaki survey were recorded on two NZNSN (New Zealand National Seismograph Network) stations: Erewhon Station (EWZ) and Otahau Downs (ODZ) (see Fig. 1). Offsets for these data range from 72 to 83 km for EWZ and 110 to 127 km for ODZ and provide crucial supplementary information on velocity and depth within the crust. Receiver gathers for both stations are shown in Fig. 4. First arrivals of Pg and Sg are identified readily on both gathers. A strong wide-angle reflection (P_lP) is clearly visible only on the ODZ receiver gather.

These arrivals can be confidently identified and are used for 2-D velocity/depth inversion. The upper crustal model, derived earlier, and a lower crustal reflector serve as a starting model. ODZ lies in the azimuth of the Reftek profile and forms its southern extension (Fig. 1). EWZ extends this 2-D profile to the north, ignoring anisotropy in the crustal rocks. This is reasonable as laboratory studies show only weak anisotropic behaviour of 2.1% in greywacke rock (Okaya et al. 1995).

The velocity/depth inversion for this reasonably simple model proves stable only for data from ODZ. If EWZ traveltime data (Pg) are included, the inversion becomes unstable for the targeted resolution of 50 ms r.m.s. error. This is considered to result from raypath differences in the near surface, introduced by station EWZ being displaced off the line of the Reftek profile. The thickness of the surface layer probably varies with direction, and small differences in thickness can produce time delays significant enough to disrupt the inversion process. Therefore, the inclusion of Pg arrivals at EWZ required an additional forward modelling step. The final velocity model (Fig. 5) gives a velocity of 6.2 km/s at 6 km depth increasing to 6.25 km/s at the lower crustal reflector of 25 km. Error estimates for the velocity values are <3%. The velocity in the lower crust is sampled only by the wide-angle reflection recorded at ODZ. If a gradual velocity reduction occurs at lower crustal depth, which would result in a shallower depth to the reflector, it could not be resolved with these data. Simulated variations in the crustal velocity affect mainly the dip of the lower crustal reflector because these data are unreversed. The error in the depth of this interface is estimated at ±1 km.

A weak and diffuse P_lP arrival is identified on the EWZ receiver gather at c. 17.5 s two-way traveltime (twtt) (Fig. 4) and contrasts with the strong reflection amplitudes recorded at ODZ. The difference in amplitude of these reflections is caused by the different offsets to the recording stations. Offset and depth to a reflecting interface affect the angle of incidence of the reflection and the resulting amplitude. The amplitude response of the P_lP reflection has been calculated as a function of incident angles using Zoeppritz's equations (Fig. 6). The calculations are based on a homogeneous two-layer model. Velocity and density values, representative for a greywacke/schist layer overlying an oceanic crustal layer (solid lines) and mantle (dashed line), are chosen. The difference in amplitude response between the two stations is evident, and is caused by the recording of subcritical reflections at EWZ, and the recording of reflections from beyond the critical angle (wide-angle) at ODZ. Strong amplitudes would also be recorded at EWZ at far offsets, if the reflection originates from a first-order Moho discontinuity. This is not observed. Therefore, these reflections are interpreted to be from an underlying oceanic layer.

The moveout of the P_lP reflection recorded at EWZ is small when compared to a reflection from a horizontal interface. There are two reasons for this: (1) the recording configuration is 3-D and is equivalent to oblique fan-shooting; (2) the reflecting plane is dipping to the northwest (as defined below in the walkaway section) such that the reflection points from far offset shots are at shallower depths than those from nearer shots. The crustal velocity model (see above) was used to simulate arrivaltimes of this event using 3-D raytracing. Predicted arrivaltimes of P_lP at EWZ are c. 0.5 s earlier than those observed. However, this difference could be accounted for by a 3% reduction in velocity or by an increase in depth of c. 1.5 km to the dipping interface. Good agreement is observed in moveout for the recorded and modelled reflection. This result is consistent with a northwest-dipping interface and substantiates the existence of a dipping and thickened continental crust towards the Southern Alps.

Apparent velocities defined for Pg and Sg are used to compute a Poisson's ratio for the greywacke basement. A significant advantage in using apparent velocities rather than

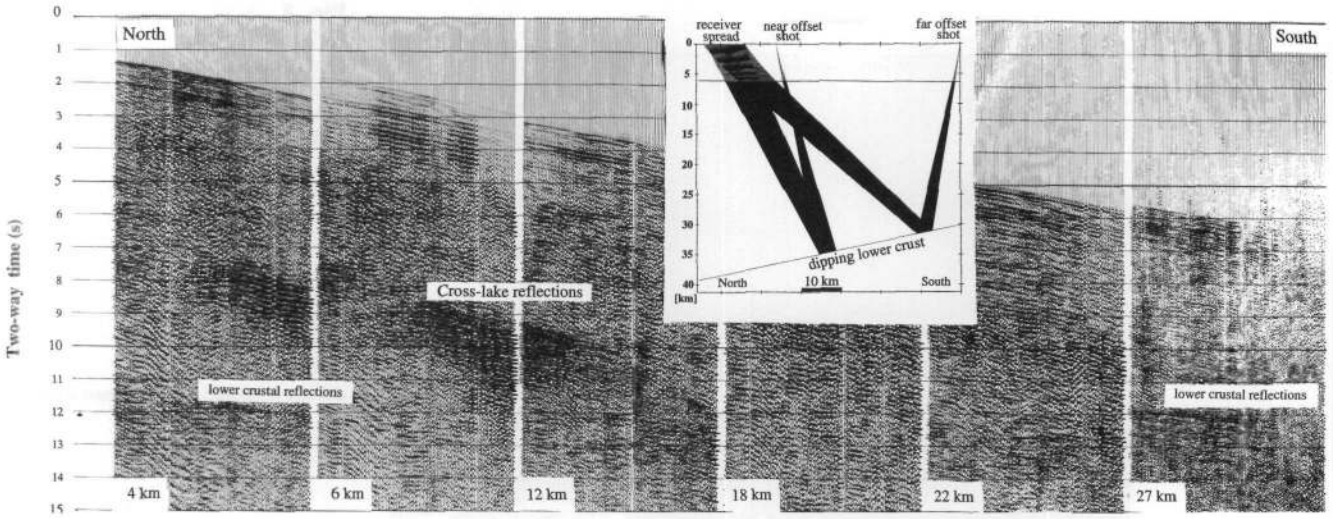

Fig. 7 Shotgathers of the walkaway spread show a lower crustal reflection at c. 11.5 s twtt. The arrivaltime is the same for all offsets, which indicates an interface dipping north at c. 15°. *Inset*: The raypaths associated with the near-offset and far-offset shots, highlighting the dipping interface. The bright spot at about 8 s twtt is believed to be caused by sideswipe; possibly by cross-lake reflective energy.

true velocities is that static effects are cancelled when identical raypaths for both types of waves are assumed. The velocities yield a Poisson's ratio of 0.21 ± 0.03 and 0.22 ± 0.03 for ODZ and EWZ, respectively. Data quality is slightly better for ODZ, and this value is taken to be representative. It is only fractionally smaller than the value of 0.25 determined in a seismicity study in the South Island by Eberhardt-Phillips (1995). However, if the lower Poisson's ratio derived here represents a deviation from a mean for greywacke crust in this region, then the difference could be attributed to the presence of unsaturated cracks in the greywacke rock. Popp & Kern (1994) found that both the P- and S-wave velocities decrease with increasing crack density, and that Poisson's ratio decreases for dry cracks and increases for saturated cracks. Such a fractured basement would also be consistent with the diffuse region of seismicity southeast of the Alpine Fault and the lack of correlation of the epicentres of these earthquakes with known faults (Eberhardt-Phillips 1995).

Walkaway profile

A walkaway survey was shot with the receiver spread fixed at the northern end of the lake and shots fired into it at offsets of 4, 6, 12, 18, 22 and 27 km to the south. In this fashion, a continuous shot-receiver record could be constructed (Fig. 7). The purpose of this was to distinguish coherent noise from signal and to attain a wide-angle aperture for deep reflections.

Distortion of wave propagation through near-surface heterogeneity is clearly manifest in the variable frequency content of the walkaway record. Also clearly visible is a multiple refracted arrival which is caused by reverberation in the water column (bubble pulse) and is generally associated with marine seismic sources (Dobrin 1981). The period of the reverberation (450 ms) is consistent with theoretical values for a charge size of 25 kg and a 20 m depth.

Strong reflections from the opposite side of the lake are recorded between 8 and 9 s twtt. Usually the cross-lake reflections are prominent only after low-cut filtering and are identified by their moveout velocity which is close to the velocity of sound in water. However, prominent differences in amplitude and frequency exist for these reflections (Fig. 7). These reflections have lower frequencies and larger amplitudes than those found for typical cross-lake reflections seen on our data. This change in signal character could be explained by a well-defined seismic discontinuity on the other side of the lake. That this event is a diffraction in the middle to lower crust can be rejected because estimates of the average velocity of 1700 ± 300 m/s to the source of such a diffraction can be obtained from the stacked seismic section (Fig. 8) using the simple relation

$$V_{avg} = \sqrt{\frac{2}{T_0 \Delta t}}\, x$$

given by Feng & McEvilly (1983). V_{avg} is the average velocity, T_0 is the two-way traveltime to the vertex of the diffraction, x is the horizontal distance from the vertex at which the time difference Δt is determined. This low velocity clearly suggests that the event is at shallow depth and of sideswipe nature.

A further reflection is observed at c. 11.5 s twtt. This reflection can be traced across the entire walkaway spread but is more prominent on the near-offset and far-offset shots. The reflection is unusual in that it arrives at approximately the same time for all offsets. This can be explained if it originates from an interface that dips northwards towards the recording spread (Fig. 7, inset) with an apparent dip of 15 ± 3° based on the velocity model (Fig. 5). Depths to the reflecting points on the interface range from 31 km for the far-offset shot (southern end) to 35 km for the near-offset shot (northern end). Such a deep interface must be associated with regional deformation and is believed to represent the downwarping of the greywacke/schist crust towards the plate boundary. If the true dip is orthogonal to the strike of the Alpine Fault, the dip increases to 18°, and only insignificant changes occur in the depth to the reflector.

CDP line

An unmigrated stacked section of the multi-channel reflection profile is shown in Fig. 8. Seismic energy reflected

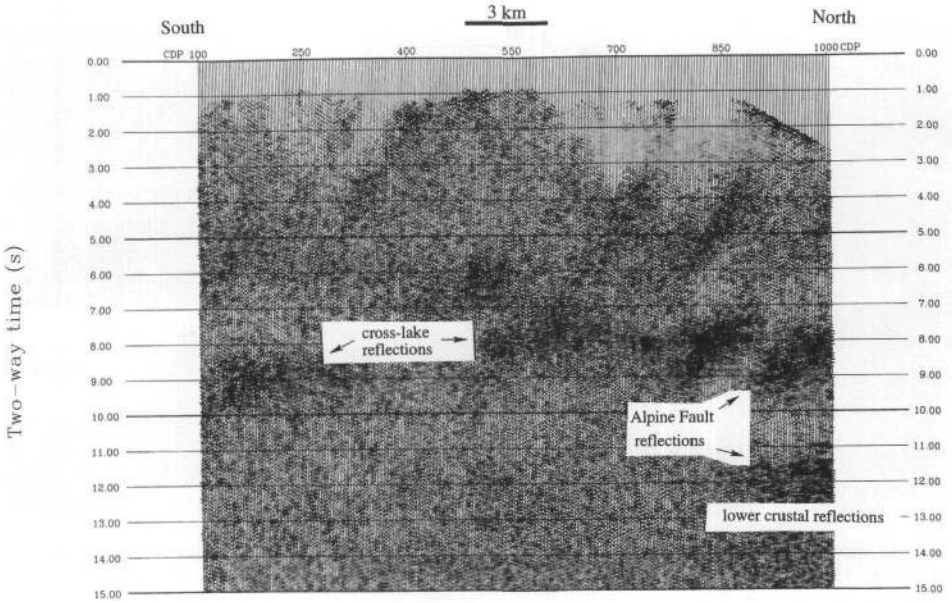

Fig. 8 Stacked section of the CMP profile exhibits a low signal-to-noise because of the attenuating character of the glacial surface layer. Energy from cross-lake reflections dominates the section at c. 7–8.5 s twtt. Improvement in reflection character can be seen at the northern end of the line where the glacial deposits are much thinner. The deep reflections at 11.7 s twtt correspond to the dipping interface identified on the walkaway spread. Steeply dipping reflections at 9 and 11.5 s twtt define a broad Alpine Fault Zone.

from the opposite side of the lake dominates the stacked seismic section between 7 and 8.5 s twtt. Due to their multicyclic character, these cross-lake reflections stack in despite their low moveout velocity.

The absence of coherent deep crustal reflections over most of the section is attributed to the low signal-to-noise ratio caused by scattering and absorption of seismic energy in the glacial surface material. Signal attenuation appears to be linked directly to the thickness of the glacial deposits. There is marked improvement in data quality where the glacial sediments thin significantly at the northern end of the line (Fig. 2). This improvement in signal-to-noise ratio is not related to processing and can also be seen clearly on the unprocessed field data. On this northern part of the section, a deep crustal reflection occurs at c. 11.7 s twtt and corresponds to the deeper event on the walkaway spread (see below). However, the lateral extent of this reflection on the stacked seismic section is too short to define a dip.

The higher signal-to-noise ratio at the northern end of the line also reveals two distinct reflections at c. 9 and 11.5 s, which dip steeply to the south. These events are highlighted in Fig. 9, which is an enlargement of the relevant portion of the seismic stacked section. The stronger reflection at 9 s twtt was recognised on the field data by Davey et al. (1995). Their analysis locates the reflection close to the plane of the Alpine Fault, assuming the strike of the reflector is parallel to the surface trace of the fault. A dip of 40 ± 5° and depth of 22 km to the reflector were calculated. The later reflection at 11.5 s twtt has not been identified previously. This reflection appears to be parallel to the dipping reflection at 9 s twtt, which suggests that both reflections arise from a similar structure.

Calculation of the reflector dip from the slope of the reflection events on the stacked seismic data indicates a lower dip than defined by Davey et al. (1995). Taking an average velocity of 6.0 km/s for the medium above the reflector, and considering the angle of 30° between the seismic profile and the reflector plane, a reflector dip of 33

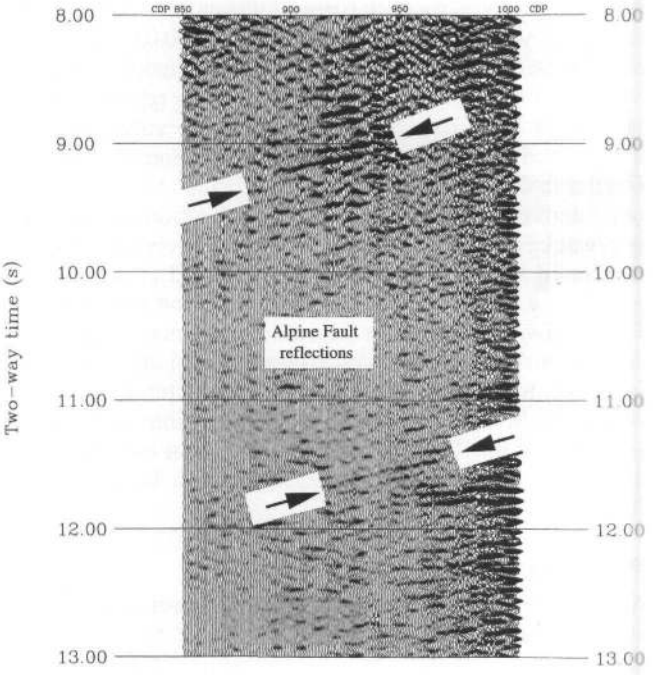

Fig. 9 Enlargement of Fig. 8 showing the steeply dipping reflections which define a broad fault zone.

± 5° results for both events. The difference between the dip value calculated from the stacked seismic data and the calculation done by Davey et al. (1995) is likely to originate from raypath complexities and/or possible deviation from a planar reflecting interface. As the reflection events on the stacked seismic section represent a summation of several reflection amplitudes, this value provides a better estimate of the true dip of the reflector. Different results are obtained if the orientation of the reflector plane is varied. However, it seems reasonable to assume that such steeply dipping reflectors are associated with a broad Alpine Fault Zone,

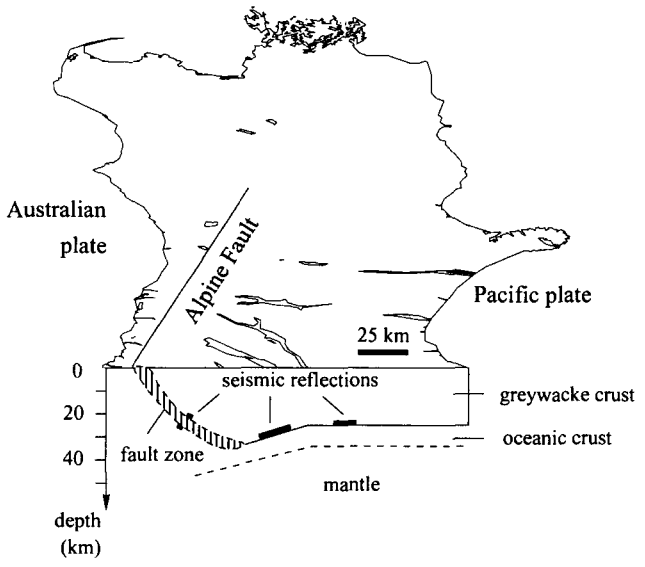

Fig. 10 Cross-sectional model of the crustal structure in the central South Island shows the 25 km thick undeformed greywacke crust to the east. Crustal thickening onsets c. 80 km east of the Alpine Fault and can be traced to a depth of 35 km. A low-velocity zone is inferred to be associated with the broad southeastward dipping Alpine Fault Zone.

and they are interpreted to mark its western and eastern boundaries.

The width of this inferred fault zone is defined by the interval velocity between both reflections. Although no direct measurement of this velocity is possible, an estimate can be obtained by comparison of seismic reflection amplitudes. The polarity of these events, which would indicate a change towards a higher or lower velocity medium, cannot be identified unambiguously. However, an amplitude ratio of about 1 is obtained between the dipping event at 9 s and the lower crustal reflection recorded at 11.7 s, which indicates similar value of the acoustic impedance contrast at both interfaces. If a velocity value of 7.1 km/s is adopted for the presumed oceanic lower crust, 6.25 km/s for the greywacke crust (see velocity model), and the relatively small density contrast is ignored, then the velocity for the material in the fault zone would be either 5.3 km/s or 7.0 km/s, depending on whether the dipping reflection at 9 s corresponds to a velocity reduction or increase. A velocity of 7.0 km/s is close to that found for the fast direction of the anisotropic schistose rock (Okaya et al. 1995). The time difference of 2.4 s between both reflections results in a width of the fault zone of c. 6.5–8.5 km at a depth of c. 25 km.

DISCUSSION

Results from the vertical incident and refraction/wide-angle reflection seismic measurements produce a first-order model of crustal structure. The reflection events, recorded from the Alpine Fault Zone and the lower crust, provide important constraints on the crustal structure in the central South Island. Accurate time to depth conversions are possible due to the well-defined velocity model obtained from explosion data recorded on the Reftek array and the National Network stations. Figure 10 summarises the results of this survey and shows a cross-section representative of the crustal structure in the central South Island.

Agreement exists between this crustal cross-section and the gravity model by Woodward (1979). Particularly striking is the resemblence between both models in the lower crustal interface dipping towards the plate boundary because it delineates the shape of the crustal root. However, despite the apparent congruence between the gravity model and this seismic model, the lower crustal interface in the gravity model represents the Moho, whereas the wide-angle reflection recorded at EWZ indicates a greywacke/schist-oceanic crustal interface. Also, any comparison needs to be treated with care because no gravitational effect of subducted mantle material has been allowed for, as discussed by Blundell et al. (1992) for the European Alps and by Stern (1995) for the Southern Alps. Variations in crustal structure must be expected in cross-sections parallel to the south and north of this profile, as can be inferred from the observed gravity anomaly over the South Island. A decrease in thickness of the greywacke-schist layer seems to occur from the Pukaki-ODZ profile towards the Canterbury Plains, where lower crustal reflections recorded near Carew (Fig. 1) indicate a greywacke-schist thickness of 21 ± 1 km (Taylor 1996). A thickness of 20 km for the greywacke-schist part of the crust has also been identified beneath North Canterbury (Reyners & Cowan 1993).

Reyners (1987) analysed crustal seismicity from data recorded on the Pukaki network over an 8 year period. He identified the occurence of earthquakes beneath the central Southern Alps at depths of up to 73 km and inferred a structure dipping towards the Alpine Fault. He produced a cross-sectional plot of earthquake hypocentres, which exhibits a V-shape structure similar to the one obtained here.

A crust/mantle boundary at 32 km depth beneath Lake Pukaki has been deduced by Calhaem et al. (1977) from S to P converted phases observed on earthquake data. Their depth value seems to be too shallow for the Moho, but a match between both data can be obtained if the origin of the phase conversion is attributed to the greywacke/schist-oceanic crustal interface.

No mid-crustal reflections are recorded on either the vertical incident data or on the wide-angle data. The absence of such reflectors opposes the interpretation of Haines et al. (1979), who attributed the occurence of mid-crustal seismicity in the Lake Pukaki region to a structural discontinuity at a depth of 9.6 km. A discrete seismic discontinuity is not necessarily required to generate earthquakes but is a prerequisite to produce seismic reflections. Our data would support the interpretation by Eberhardt-Phillips (1995) that crustal seismicity results from fracturing in the greywacke basement.

Rays of Pg and Sg sampled the average velocity of greywacke basement at depths approximately corresponding to the depth of crustal seismicity. If one accepts that the calculated low value of Poisson's ratio reflects a deviation from the normal Vp/Vs ratio, then this could be attributed to fracturing in the crust.

The reflections from the Alpine Fault Zone image only a limited extent of the dipping interfaces. If they are planar, and extrapolated upwards, they intersect the surface west of the Alpine Fault, which suggests that the fault zone steepens towards the surface. Although a range of possible interval velocities for the proposed fault zone can be estimated from amplitude ratios, the physical properties of the material

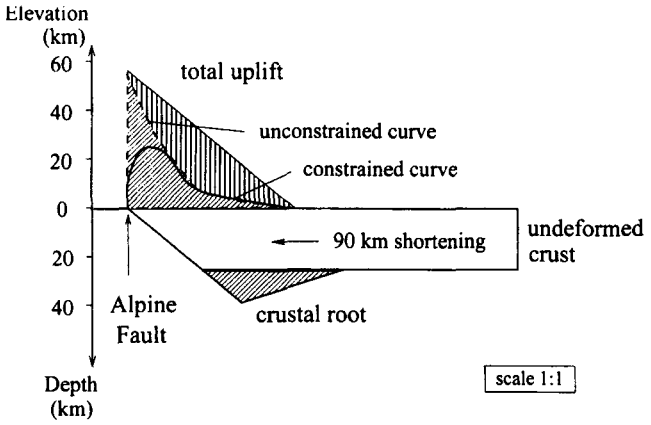

Fig. 11 The area of total uplift (triangle) is calculated from the difference of material lost due to 90 km of crustal shortening and material which now forms the crustal root. Also shown are the constrained and unconstrained curves of total uplift defined by Adams (1979). The unconstrained exponential uplift curve accounts for only half the material which has been uplifted.

which causes the reflectivity are not well constrained. Possible explanations for the reflectivity are: (1) a zone of mylonites; (2) a change in rock type from greywacke to schist; (3) an increase in pore pressure due to fluid saturation. For (1), Fountain et al. (1984) showed that mylonites can extend to great depths and cause lower crustal reflections. Mylonitic rocks are found as outcrops adjacent to the Alpine Fault. For (2), evidence from anisotropy studies (Okaya et al. 1995) suggests that rays impinging at a high angle onto the plane of foliation of the schist provide a sufficient acoustic impedance contrast to generate reflections. For (3), the presence of fluids at mid-crustal depths, based on electrical conductivity studies, has been suggested by Ingham (1995). This could result in a low-velocity zone (LVZ) as postulated by Smith et al. (1995). A high to low velocity boundary would result in a reversal of the waveform for the reflection at 9 s twtt. This was not resolvable on our data. A LVZ has been identified in the vicinity of the San Andreas Fault in California (Feng & McEvilly 1983) but its cause has not been identified.

The total amount of material that has been subjected to uplift can be estimated from the amount of crustal shortening and the material which delineates the crustal root identified in this study. To derive such an estimate, we assume that the total amount of uplift can be derived from the difference between material lost due to crustal shortening and material which now forms the crustal root. This implies that no crustal material has been subducted.

In a recent paper on plate reconstruction, Walcott (in press) ascribes 90 ± 10 km of crustal shortening to the central South Island. This value is equivalent to a cross-sectional area of 1800–2250 km^2 of crustal material lost in the deformation processes for an undeformed crust of 20 and 25 km thick, respectively. The crustal root in Fig. 10 is approximated by a triangular geometry with an equivalent area (Fig. 11). The area of this crustal root also varies with thickness of the undeformed crust, and ranges from 370 to 700 km^2 for a thickness of 25 and 20 km, respectively. From these values, a total amount of 2-D uplift of 1100–1880 km^2 is calculated. Figure 11 outlines this basic principle for a 25 km thick undeformed crust.

This result strongly contrasts previous estimates of uplift (Adams 1979; Allis 1986; Kamp et al. 1989). For comparison, uplift curves from Adams (1979) are included in Fig. 11. Adams (1979) expressed the total amount of uplifted material numerically by the exponential function

$$U_t = 55e^{-0.065x} - 45e^{-0.2x}$$

U_t describes the total uplift and x the distance to the east of the Alpine Fault. The second term constrains uplift by vertical drag on the Alpine Fault (solid line in Fig. 11). The first term of this equation provides an unconstrained uplift curve (dahsed line in Fig. 11), which is larger than uplift curves derived, for example, by Allis (1986), Kamp et al. (1989), and Grapes (1995). The unconstrained curve describes an area of 846 km^2, which is smaller by a factor of up to 2 compared to the amount of total uplift calculated here. This indicates either that uplift rates are generally larger or that uplift does not decay exponentially with distance from the Alpine Fault, or both.

CONCLUSION

A crustal depth/velocity structure has been derived for the central South Island from the Lake Pukaki seismic experiment. P-wave velocities are well constrained and show a velocity gradient in the upper 6 km for the greywacke rock with a smooth transition into a constant velocity of c. 6.2 km/s below. The greywacke/schist portion of the crust beneath the Kirkliston Range is c. 25 km thick.

Crustal thickening initiates at a distance of c. 80 km from the Alpine Fault and can be traced to a depth of 35 km. The boundary of the Australian-Pacific plate in the central South Island, often identified as a single interface by the Alpine Fault, is modelled as a 7.5 km broad zone at c. 25 km depth which is likely to exhibit low seismic velocities.

A Poisson's ratio of 0.21 ± 0.03 is determined for the greywacke basement in the central South Island. This relatively low value is interpreted tentatively to reflect fracturing in the crust and would be consistent with the diffuse seismicity observed in central South Island.

The calculated amount of material which has been subjected to uplift is larger than described by uplift curves in previous studies. To accommodate this amount of uplift requires a different distribution of uplift southeast of the Alpine Fault.

ACKNOWLEDGMENTS

This project was supported by the Foundation for Research, Science and Technology, the Institute of Geological & Nuclear Sciences, and Victoria University of Wellington. Support for this project was also provided by the U.S. National Science Foundation through the Continental Dynamics Program grant EAR-9418530. This paper benefited substantially from suggestions and comments made by Bruce Goleby and an unnamed reviewer. We are grateful to the seismic crew for their help with the recording of the field data. We thank Mark Chadwick for converting the data recorded on the seismological network stations, and Michelle Robertson for her help with the reduction of the Reftek data.

REFERENCES

Adams, C. 1979: Age and origin of the Southern Alps. *In*: Walcott, R. I.; Cresswell, M. M. *ed.* The origin of the Southern Alps. *The Royal Society of New Zealand bulletin 18*: 73–77.

Allis, R. G. 1986: Mode of crustal shortening adjacent to the Alpine Fault, New Zealand. *Tectonics 5 (1)*: 15–32.

Blundell, D.; Freeman, R.; Mueller, S. 1992: A continent revealed, the European Geotraverse. Cambridge, Cambridge University Press.

Calhaem, I. M.; Haines, A. J.; Lowry, M. A. 1977: An intermediate depth earthquake in the central South Island used to determine a local crustal thickness. *New Zealand journal of geology and geophysics 20*: 353–361.

Davey, F. J.; Henyey, T.; Kleffmann, S.; Melhuish, A.; Okaya, D.; Stern, T. A.; Woodward, D. J. and others 1995: Crustal reflections from the Alpine Fault Zone, South Island, New Zealand. *New Zealand journal of geology and geophysics 38*: 601–604.

Dobrin, M. B. 1981: Introduction to geophysical prospecting. London, McGraw Hill.

Eberhardt-Phillips, D. 1995: Examination of seismicity in the central Alpine Fault region, South Island, New Zealand. *New Zealand journal of geology and geophysics 38*: 571–578.

Farrell, R. C.; Euwema, R. N. 1984: Refraction statics. *Proceedings of the IEEE 72(2)*: 1316–1329.

Feng, R.; McEvilly, T. V. 1983: Interpretation of seismic reflection profiling data for the structure of the San Andreas fault zone. *Bulletin of the Seismological Society of America 73 (6)*: 1701–1720.

Fountain, D. M.; Hurich, C. A.; Smithson, S. B. 1984: Seismic reflectivity of mylonite zones in the crust. *Geology 12*: 195–198.

Gair, H. S. 1967: Sheet 20—Mt Cook. Geological map of New Zealand. Lower Hutt, New Zealand Geological Survey, Department of Scientific and Industrial Research.

Grapes, R. H. 1995: Uplift and exhumation of alpine schists, Southern Alps, New Zealand: thermobarometric constraints. *New Zealand journal of geology and geophysics 38*: 525–533.

Haines, A. J.; Calhaem, I. M.; Ware, D. E. 1979: Crustal seismicity near Lake Pukaki, South Island. *In*: Walcott, R. I.; Cresswell, M. M. *ed.* The origin of the Southern Alps. *The Royal Society of New Zealand bulletin 18*: 87–94.

Henyey, T.; Stern, T.; Molnar, P. 1993: A plan for the geophysical survey of the Southern Alpine Orogen, New Zealand: an oblique-convergent continent-continent collision. *Transactions of the American Geophysical Society (EOS) 74*: 316–317.

Ingham, M. A. 1995: Electrical structure along a transect of the central South Island, New Zealand. *New Zealand journal of geology and geophysics 38*: 559–563.

Kamp, P. J. J.; Green, P. F.; White, S. T. 1989: Fission track analysis reveals character of collisional tectonics in New Zealand. *Tectonics 8 (2)*: 169–195.

Kleffmann, S. 1994: Effects of surficial till on seismic reflection data. Unpublished MSc thesis, Research School of Earth Sciences, Victoria University of Wellington, Wellington, New Zealand.

Langdale, S. 1996: Late Tertiary deformation in Cannington Basin, South Canterbury: evidence from seismic and gravity data. Unpublished BSc Hons thesis, lodged in the Library, Victoria University of Wellington, Wellington, New Zealand.

Melhuish, A.; Kleffmann, S. 1995: Acquisition and preliminary processing of deep crustal seismic data at Lake Pukaki, central South Island. *Institute of Geological & Nuclear Sciences technical report 95/37.*

Molnar, P.; Atwater, T.; Mammerickx, J.; Smith, S. M. 1975: Magnetic anomalies, bathymetry and the tectonic evolution of the South Pacific since the Late Cretaceous. *Geophysical journal of the Royal Astronomical Society 40*: 383–420.

Norris, R. J.; Koons, P. O.; Cooper, A. F. 1990: The obliquely-convergent plate boundary in the South Island of New Zealand: implications for ancient collision zones. *Journal of structural geology 12 (5/6)*: 715–725.

Okaya, D.; Christensen, N.; Stanley, N.; Stern, T. 1995: Crustal anisotropy in the vicinity of the Alpine Fault, South Island, New Zealand. *New Zealand journal of geology and geophysics 38*: 579–583.

Pearson, C. F.; Beavan, J.; Darby, D.; Blick, G. H.; Walcott, R. I. 1995: Strain distribution across the Australian-Pacific plate boundary in the central South Island, New Zealand, from GPS and earlier terrestrial observations. *Journal of geophysical research 100 (B11)*: 22071–22081.

Popp, T.; Kern, H. 1994: The influence of dry and water saturated cracks on seismic velocities of crustal rocks—a comparison of experimental data with theoretical model. *Surveys in geophysics 15*: 443–465.

Reyners, M. 1987: Subcrustal earthquakes in the central South Island, New Zealand, and the root of the Southern Alps. *Geology 15*: 1168–1171.

Reyners, M.; Cowan, H. 1993: A transition from subduction to continental collision: crustal structure in the North Canterbury, New Zealand. *Geophysical journal international 115*: 1124–1136.

Smith, E. G. C.; Stern, T.; O'Brien, B. 1995: A seismic velocity profile across the central South Island, New Zealand, from explosion data. *New Zealand journal of geology and geophysics 38*: 565–570.

Speight, J. G. 1963: Late Pleistocene historical geomorphology of the Lake Pukaki area, New Zealand. *New Zealand journal of geology and geophysics 6*: 160–188.

Stern, T. 1995: Gravity anomalies and crustal loading at and adjacent to the Alpine Fault, New Zealand. *New Zealand journal of geology and geophysics 38*: 593–600.

Suggate, R. P.; Stevens, G. R.; Te Punga, M. T. 1978: The geology of New Zealand. Wellington, New Zealand. Government Printer.

Taylor, L. 1996: SIGHT: Forward modelling and high resolution vignettes. Unpublished DipAppSc in Geophysics thesis, lodged in the Library, Victoria University of Wellington, Wellington, New Zealand.

Walcott, R. I. 1978: Present tectonics and late Cenozoic evolution of New Zealand. *Geophysical journal of the Royal Astronomical Society 52*: 137–164.

Walcott, R. I. in press: Modes of oblique compression: Late Cenozoic tectonics of the South Island of New Zealand. *Reviews of geophysics 36(1).*

Wellman, H. W. 1953: Data for the study of recent and late Pleistocene faulting in the South Island of New Zealand. *New Zealand journal of science and technology B34*: 270–288.

Wellman, H. W. 1979: An uplift map for the South Island of New Zealand, and a model for uplift of the Southern Alps. *In*: Walcott, R. I.; Cresswell, M. M. *ed.* Origin of the Southern Alps. *The Royal Society of New Zealand bulletin 18*: 5–12.

Woodward, D. J. 1979: The crustal structure of the Southern Alps, New Zealand, as determined by gravity. *In*: Walcott, R. I.; Cresswell, M. M. *ed.* Origin of the Southern Alps. *The Royal Society of New Zealand bulletin 18*: 95–98.

Zelt, C. A.; Smith, R. B. 1992: Seismic traveltime inversion for 2-D crustal velocity structure. *Geophysical journal international 108*: 16–34.